

SHORT THESIS FOR THE DEGREE OF DOCTOR OF PHILOSOPHY (PHD)

Cellular adaptation to hypoxia in classic Hodgkin lymphoma

by Orsolya Matolay

Supervisor: Gábor Méhes, Ph.D., D.Sc.



UNIVERSITY OF DEBRECEN

DOCTORAL SCHOOL OF CLINICAL MEDICINE

DEBRECEN, 2022

Cellular adaptation to hypoxia in classical Hodgkin lymphoma

By: Orsolya Matolay

Supervisor: Gábor Méhes, Ph.D., D.Sc.

Doctoral School of Clinical Medicine, University of Debrecen

Head of the **Defense Committee:** Gabriella Szűcs, Ph.D., D.Sc.

Reviewers: Csongor Kiss, Ph.D., D.Sc.

Ágota Szepesi, Ph.D.

Members of the Defense Committee: Katalin Erdélyi, Ph.D.

András Mádi, Ph.D.

The PhD Defense will be online on 16th June 2022 1.p.m.

Live online access will be provided. If you wish to join the discussion, please send an e-mail to the Orsolya.matolay@med.unideb.hu address until 2 p.m at latest on the previous day of the defense (15th June, 2022). After the deadline, for technical reasons, it is no longer possible to join in to the defense.

2022

1 Introduction

Lymphomas are a group of malignancies that arise from components of the immune system, usually affecting the T- and B-cells. Hodgkin's lymphoma (HL) represents approximately 10% of all lymphomas, thus it is one of the rare monoclonal hematopoietic malignancies with B-cell origin. HL continues to elude researchers and clinicians concerning the etiology, mechanism of malignant transformation. According to the 2008 WHO Classification and revision in 2016 HL could be further divided into two main groups: nodular lymphocyte-predominant Hodgkin's lymphoma (NLPHL) and classic Hodgkin's lymphoma (cHL). cHL accounts for approximately 85% of all HL. cHL can be further subdivided into four histological variants: nodular sclerosis (NS), mixed cellularity (MC), lymphocyte rich (LR), and lymphocyte depleted (LD) subtype. cHL is characterized by a rare, malignant cell type known as the Hodgkin-Sternberg-Reed cell (HRS). The large mononucleated Hodgkin cell and the large multinucleated Reed- Sternberg (RS) cells coexist with a non-neoplastic cell population.

Hypoxia is defined as reduced tissue oxygen partial pressure (pO_2) levels than physiological levels. This can occur due to hypoperfusion or increased cellular demand for molecular oxygen that exceeds vascular supply, leading to a bioenergetic crisis. Hypoxia may develop at an early stage of tumor progression and it has a profound impact on many aspects of tumor biology, inducing signaling pathways in neoplastic cells that allow them to survive under low oxygen tension. Hypoxia can induce several adaptive mechanisms, which fall under a key transcriptional factor, the Hypoxia Inducible transcriptional factor (HIF). HIF1 α mediates many aspects of cellular homeostasis and the transcriptional activation of the factor leads to metabolic shift. In conditions with reduced oxygen levels or the absence of oxygen, the cells will switch over to glycolysis to maintain cellular energy supply. Neoplastic cells may continue glycolysis even under normoxic conditions, the phenomenon is called the Warburg effect.

However, glucose catabolism also results in the accumulation of several metabolic end products, including CO_2 , protons, and lactic acid. Prolonged accumulation of these substances may lead to intracellular acidosis that interferes with biosynthetic reactions and signaling because most of the molecules, regulators and other components of cellular machinery are pH-sensitive. To avoid cytosolic acidification, cells redirect the ion flux and increase the rate of pH-regulating activity. Due to the active upregulation of transmembrane enzymes or channels, the intracellular pH (pHi) returns to near alkaline values that support cell survival

and proliferation. The mechanism of enzymes is generally based on the diffusion of CO₂, export of lactate and H⁺, and the hydration of CO₂ to produce bicarbonate ions.

Carbonic anhydrase IX (CAIX), a highly HIF1 α -dependent enzyme- has an important role in acid-base balance as it actively catalyzes the elimination of the H⁺ in order to restore physiological intracellular pH, while extracellular pH becomes acidotic. That would support the survival of cancer cells despite the hostile microenvironment and facilitate tumor cell invasion. The CAIX-related adaptive response is associated with aggressive tumor phenotype and resistance to chemotherapy.

Hypoxia may already develop at an early stage of tumor progression and exerts a pivotal impact on many aspects of cancer biology. In a hypoxic niche, the neoplastic cells must undergo metabolic adaptation in order to survive. Previous studies have concluded that mature B-cells can turn into cells with key HRS cell characteristics in hypoxic conditions and hypoxia also influences drug resistance. The daily histopathology routine frequently reflects tissue changes suggesting hypoxic damage in association with other aggressive features.

Previous studies concluded that hypoxia induces atypia similar to HRS-cells in mature B-cells and induces drug resistance, however, data are generally missing about the hypoxia-induced metabolic adaptation and pH-regulation in cHL.

2 Objectives

2.1 Quantitative analysis of CAIX enzyme expression in cHL patient samples

In this study, we aimed to examine biopsy samples from cHL patients to have an insight into the complexity of the hypoxia-related changes, expression of CAIX, and its role in the progression of lymphomas. We wanted to assess how the expression of CAIX correlates with patient survival and other clinical parameters (e.g. age, gender, relapse, response to therapy). Besides light microscopy, we wanted to assess a set of selected cases with digital image analysis using QuantCenter, DensitoQuant module with a scoring algorithm developed and validated by 3DHistech, Budapest, Hungary.

2.2 Occurrence and dynamics of CAIX in experimental cHL models

We aimed to examine the distinct interplay between hypoxia-associated altered adaptation, expression of cell kinetic factors, markers, and response to therapy in hypoxia in cHL cell cultures.

For this purpose:

- We characterized and validated the L1236 and L428 human Hodgkin's lymphoma cell lines.
- We determined the effect of hypoxia through the expression of several HIF1 α downstream effectors at the mRNA and protein expression levels.
- We performed experiments to address the *in vitro* response – efficiency and efficacy – to the common therapeutic drug combination ABVD in normoxia and hypoxia.

3 Materials and methods

3.1 Sample selection and immunohistochemical analysis

cHL cases were identified from the period between 1999 and 2019 diagnosed at the Departments of Pathology, Clinical Centre, University of Debrecen, and at the J6sa Andr6s Teaching Hospital, Ny6regyh6za, Hungary. Histological diagnosis of cHL was reviewed according to the latest WHO classification, cases with larger quantities of pathognomic HRS-cells were identified to enable further analyses. Tissue samples were evaluated by routine pathological staining (hematoxylin-eosin - HE) for tissue characteristics (stroma, necrosis, etc.), and the IHC panel PAX5, CD20, and CD30, LMP-1, and LCA was regularly done. IHC was done on serial sections using the antibody clone Ber-H2 (Dako-Agilent, Glopsrup, Danemark) for CD30 and rabbit polyclonal antibody clones for CAIX. EnVision Flex horseradish peroxidase/diaminobenzidine (HRP/DAB)⁺ chromogen detection system (Dako-Agilent) was used to show the specific antibody binding, followed by antigen retrieval at pH 9.0. As CAIX negative control NLPHL samples, and as CAIX positive control, we used renal cell cancer.

A dual immunohistochemical reaction was assessed to examine the expression of MIB1 and CAIX. Firstly, the nuclear MIB1 was specifically labeled and detected by EnVision Flex HRP/DAB⁺, followed by a second incubation with CAIX antibody. CAIX was visualized with Flex HRP system using violet VIP chromogen (Vector Laboratories, Burlingame, CA, USA). Methyl-green solution (Vector Laboratories) was used to counterstain unlabeled cell nuclei.

CAIX immunohistochemical staining was performed with both poly- and monoclonal antibodies. The immunohistochemical staining was performed according to the manufacturer's protocol and for visualization diaminobenzidine (DAB) chromogen was used.

3.1.1 Immunocytochemistry

Cell culture-derived cytospin preparations were fixed in 10% formaldehyde, after washing them once in PBS. A droplet of cells was placed on glass slides, followed by 24h fixation time, then they were let to dry (1 h). For immunohistochemistry, the protocol of BenchMark ULTRA was used. Staining was performed in a BenchMark Ultra immunostainer (Roche Diagnostics, Germany). OptiView DAB IHC Detection kit and UltraView Universal DAB Detection kit were

used to show specific antibody binding, after antibody retrieval. The intensity and distribution of CAIX, CAXII, HIF1 α , GLUT1, MIB1 expression were assessed by light microscopy (DM2500 microscope, Leica, Wetzlar, Germany) and then digitalized with Panoramic MIDI Slide Scanner (3D Histech, Budapest, Hungary). For semi-quantitative analysis, we used the DensitoQuant module of QuantCenter Software 2. (3D Histech, Budapest, Hungary) after the application of manually added annotations. Double staining for MIB1-CAIX was also performed.

3.2 Digital image analysis

Only the representative CD30 and CAIX lymph node samples were used for digital analyses. CD30 and CAIX are membrane-associated proteins, therefore both can be analyzed using the same software. The slides were scanned with Panoramic Slide Scanner MIDI automatic (3DHistech, Budapest, Hungary). Manual annotations were applied with the use of Caseviewer 2.2. Software (3DHistech, Budapest, Hungary). We applied free-hand annotations and we excluded the damaged areas (e.g. artifacts, gum residues, air bubbles, strong background reaction. tissue folds) to avoid false positivity. CD30 and CAIX expressions were quantitatively analyzed with QuantCenter software (3DHistech, Budapest, Hungary) and whole slide digital image analysis was performed with the DensitoQuant module. With the DensitoQuant module, we were able to perform a stain-intensity-based analysis. The module provided a fast, objective, and semiquantitative analysis by identifying the positive stain through individual positive pixels. In the module, blue and brown tolerance, color intensity, score levels, contrast, and gamma can be altered. With this method, the software was able to calculate a histoscore (H-score) based on the proportion of positive and negative pixels identified within the digitalized slide. After the analyses, the negative pixels were represented with blue color, while the positivity was represented with a spectrum of colors: the less positive was yellow, while the strong positivity was shown to be red.

3.3 Cell culture

L1236 and L428 cell lines were obtained from DSMZ (Deutsche Sammlung von Mikroorganismen und Zellkulturen GmbH/German Collection of Microorganisms and Cell Cultures, Braunschweig, Germany).

The cells were centrifugated at 1200 rpm for 5 minutes and then resuspended in an appropriate volume of fresh medium every 2-3 days. The cells were maintained in RPMI-1640 (Sigma-Aldrich, R5886) medium containing 10% FBS, 1% penicillin/streptomycin, 2 mM L-glutamine, and 1% pyruvate at 37°C with 5% CO₂.

Before analyses, we determined the cell number with the use of trypan blue. The experiments were carried out under normoxic and hypoxic conditions. Hypoxic gas mixture contained 1% O₂, 94% N₂, 5% CO₂. The gas tank was purchased by Linde.

3.4 Chemicals for *in vitro* experiments

We used the chemicals in the following concentrations:

- Doxorubicin: 0,01 µM
- Vinblastine: 1 µg/mL
- Bleomycin: 10 µg/mL
- Dacarbazine: 250 µg/mL
- Acetazolamide: 50 µM.

3.5 Detection of cell death – Propidium iodide (PI) uptake

Cells were seeded in a 24-well plate (60.000 cells/well) and they were treated with various concentrations of drugs under normoxic and hypoxic conditions. After the above-mentioned treatment, the cells were stained with 100 µL/mL propidium iodide (PI) for 30 minutes at 37°C. Cells were collected in FACS tubes, cells were washed with PBS and collected in the same FACS tubes (PBS 1:1). Then the number of the dead cells was measured by flow cytometry (FACS Calibur, BD Biosciences) and analyzed using Flowing Software 2.5.1.

3.6 Apoptosis detection using Annexin-V-FITC staining

L1236 and L428 cells were seeded in a 24-well plate (60.000 cells/well) and they were treated with various concentrations of drugs under normoxic and hypoxic conditions. After the above-mentioned treatment, the cells were stained with 100 μ L/mL propidium iodide (PI) and 5 μ L FITC Annexin V (Component A) for 1 hour on ice in darkness. Cells were collected in FACS tubes, cells were washed with PBS and collected in the same FACS tubes (PBS 1:1). Then the number of the dead cells was measured by flow cytometry (FACS Calibur, BD Biosciences) and analyzed using Flowing Software 2.5.1.

3.7 Measuring the hypoxia-related changes

3.7.1 mRNA isolation and RT-qPCR

Total RNA from cells was prepared using TRIzol reagent (Invitrogen, TR118), 2 μ g RNA was reverse transcribed using High Capacity cDNA Reverse Transcription kit (Applied Biosystems, Foster City, CA, USA, 4368813) according to the manufacturer's protocol. qPCR BIO SyGreen Lo-ROX Supermix (PCR Biosystems Ltd., London, UK, PB20.11-05) was used for the RT-qPCR reactions, the expression level of the genes was detected with Light-Cycler 480 Detection System (Roche Applied Science). A geometric mean of 36B4 and GAPDH and cyclophilin A was used for normalization.

3.7.2 Flow cytometry

CAIX expression was determined with APC Conjugation Lightning-Link[®] (ab201807) kit and Mab75 antibody (dilution: 1:1000). Briefly, L1236 and L428 cells were seeded into a T25 flask (10⁶ cells) and incubated for 48h under normoxic and hypoxic conditions followed by washing with PBS and centrifugation at 1000 RPM for 5 minutes, room temperature. After the removal of PBS, cells were fixed in 1% formalin. Formalin was washed out from the samples with HEPES and then the APC Conjugation Lightning-Link kit was used according to the manufacturer's protocol. CAIX expression was analyzed by flow cytometry (Novocyte Flow Cytometer, ACEA Biosciences, Inc., San Diego, CA, USA). Data analysis was carried out by NovoExpress[®] software (1.3.0, ACEA Biosciences, Inc., San Diego, CA, USA, 2018).

3.7.3 Statistical analysis

Histoscore is calculated with the following formula:

H-score = ((1 × % weakly stained cells) + (2 × % moderately stained cells) + (3 × % strongly stained cells)). The range of histoscore is between 0-300. In our statistical analysis, we used a non-parametric Wilcoxon signed-rank test for the comparison of two groups, unless stated otherwise. Mann-Whitney U-test was applied for group-based comparisons. Non-parametric Spearman correlation and non-parametric Kruskal-Wallis calculations were carried out to analyze the value differences in matched CD30 and CAIX cases. Data are presented as average ± SD unless stated otherwise. Statistical analysis was done using GraphPad Prism 6 software (La Jolla, CA, USA). Differences between control and treated groups were considered statistically significant at $p < 0.05$, $p < 0.01$, $p < 0.001$, respectively.

4 Results

4.1 Investigation of CAIX and CAXII expression in cHL

To quantify the CD30+, CAIX+, and CAXII+ tumor burden, serial tissue sections were examined with CD30, CAIX, and CAXII immunohistochemical staining. CD30 and CAIX expression showed to be specific for the pathognomonic HRS cells, however, CAXII expression showed to be not specific for the HRS-cells and preferably having a stromal reaction. Virtually, no other cell type but HRS proved to be positive for CAIX, having a strong membrane and/or weak cytoplasmic positivity. 56/101 (55,4%) cases were CAIX positive, the rest of our study cohort was labeled as negative cases. Necrosis was detected in only 27/101 (26.7%) cases, of which were NS 20/27 (74.07%), 4/27 (14.81%) was MC, and 3/27 (11.11%) LD, but 85% (23/27) of the evaluated samples proved to be CAIX positive. Necrotic foci were typically surrounded by a rim of CAIX positive cells. The observed phenomenon was consistent with the current literature of CAIX expression, representing the adaptation zone surrounding the necrotic core. In our cohort, the most frequent histological subtype was the NS (70/101, 69.3%), followed by MC (20/101, 19.8%) and LR (7/101, 6.9%), then LD (4/101, 0.39%). CAIX expression was positive in 56/101 (55.44%) cases, the majority of which (46/70, 65.7%) was found in the NS subtype, while in the case of MC, the positive cases were only 20% (4/20) of all MC cases. In LR the positivity was low too (2/7, 28%), on the other hand, the most aggressive clinical variant LD proved to be the highest positivity rate 100% (4/4).

MIB1 expression was also examined in cHL cases. Dual immunohistochemical staining was performed in 26 cases. According to our results, MIB1 values proved to be significantly lower in the CAIX positive population compared to the CAIX negative population ($p < 0.001$), which may indicate the CAIX positive cases are in an adaptation-related cell cycle arrest.

4.2 Digital analysis - Quantification of CD30 and CAIX expression in cHL

101 samples were examined with the digital analysis method. Manual annotations were applied, then the samples were analyzed with QuantCenter Software (3Dhistech, Budapest, Hungary), DensitoQuant module, which can calculate an H-score automatically. The cut-off

level was defined at H-score 1. The cut-off level was never reached in negative cases that validated the study.

CD30 scores showed to be highly variable, in contrast to the CAIX values which showed to be generally low but proved to be significantly higher in positive samples compared to negative cases. To identify the cell clusters, we compared the CD30+ tumor mass with CAIX- and CAIX+ total amounts. In CAIX- cases – interestingly – there was a significantly lower expression of CD30, however, in CAIX+ cases the total amount of CD30 increased.

4.2.1 Relation between CD30 and CAIX

In most of the cases the CD30 positive tumor mass was higher in CAIX+ cases, compared to CAIX- cases, however, there was no positive correlation between these factors. CAIX expression proved to be highly variable, and generally low compared to CD30 expression. It may suggest that the partial upregulation of the enzyme according to the functional diversity of the HRS cell subpopulation, as CAIX overexpression is a feature of the malignant cell compartment, while the accompanying cellular background remained negative. The minimum score for CD30 was 3.46, and the maximum was 151.33 (mean 52.37 ± 30.74), while in CAIX the minimum was 2.16 and the maximum was 90.4 (mean 18.7 ± 18.8). According to the statistical analysis, the CD30+ cell mass proved to be significantly higher, which was associated with a higher CAIX+ fraction ($p= 0.008$). According to our pixel-based analysis, the CD30 expression was the highest in the LD variant ($n = 4$, range: 24.29–109.95, mean: 63.1 ± 32.9), which was followed by NS ($n= 70$, range: 2.16–128.3, mean: 46.85 ± 27.5), MC ($n = 20$, range: 3.38–151.3, mean: 45.65 ± 35.2) and LR subtype, as expected ($n = 7$, range: 2.518–28.5, mean: 17.5 ± 8.8). The H-score range in the case of CAIX negative cases was 0.01 – 0.99 (mean 0.37 ± 0.29), and the CD30 H-score in CAIX negative cases was between 3.38 and 118.2 (mean: 37.38 ± 25.34). In CAIX positive cases the H-score was between 2.16–90.36 while the positive cases CD30 H-score was 3.46–151.33 (mean 52.37 ± 30.74). The pixel-based analysis showed that CAIX means expression was the highest in the LD variant, followed by NS, MC, and LR subtype. According to the statistical analysis, the CD30+ cell mass proved to be significantly higher, which was associated with a higher CAIX+ fraction ($p < 0.0001$). As a negative control, we used CD30 and CAIX double negative NLPHL cases ($n=8$). The significant difference between the CD30+ tumor burden in CAIX+ and CAIX- cases indicates that CAIX upregulation

occurs in progressive forms of cHL, which is tempting to speculate that the HRS-cells have a survival advantage in comparison with other cells. However, the CD30+ cell mass was increased in the CAIX+ cases, according to the correlation analysis, there was no positive correlation between these markers (p-value = 0.475, Spearman rs: -0.008).

To describe intratumor variability, a relative positivity rate was calculated for all cHL variants. CAIX/CD30 mean ratio was 0.23 ± 0.57 for all cases and 0.35 ± 0.61 for all CAIX+ cases. CAIX/CD30 ratio was the highest in LD (0.87) subtype, followed by NS (0.35), MC (0.13) and LR variant (0.83). In the LR subtype, the CAIX/CD30 ratio remained to be high, but the low number of cases (n=2) and frequency of positive events within the samples did not allow further statistical analysis.

To sum our digital image analysis up: CAIX+ cells are a subfraction of CD30 positive cells and indicate a significant functional heterogeneity within the malignant clone, which may contribute to an aggressive and resistant tumor cell phenotype.

4.3 Clinical impact of CAIX

47.5% of the patients were female (48/101) and 30/48 (62.5%) proved to be CAIX positive. In the case of male patients (53/101, 52.47%) 49% was CAIX positive (26/53). 86.13% (87/101) of our patients were over the age of 60. 48/101 (47,52%) patients complained about B-symptoms of which 60.4% (29/48) proved to be CAIX positive cases.

CAIX expression showed to have a close link with necrotic areas. While necrosis did not influence the overall survival, in the case of CAIX expression there was a minimal difference between the CAIX positive and CAIX negative cases, because the progression-free survival proved to be statistically different. Survival analysis was performed for 72 months (n=81). The overall survival (OS) rate was 0.823 and the progression-free survival (PFS) was 0.504 for the analyzed study population. Kaplan-Meier curves and Mantel-Cox statistic analysis showed that necrosis – absence or presence – did not influence the overall survival (0.812 versus 0.833, p=0.469) however, there was a mild difference between the two groups in PFS (0.19 versus 0.579, p=0.146). However, a significant difference was found in CAIX expression. The OS differed minimally between the CAIX negative and positive cases (0.934 versus 0.699, p=0.097, not significant), but in PFS there was a striking difference between the groups. According to

our analysis, there was a statistically significant longer cumulative PFS in the CAIX negative group compared to CAIX positive cases (0.771 vs 0.19, $p < 0.001$). In the case of CAIX positivity, the positive predictive value (PPV) for initial treatment failure proved to be 0.76. The negative predictive value (NPV) for CAIX negativity proved to be 0.66 ($p < 0.003$). These results suggest that the expression of CAIX elevates the likelihood of failure/progression after initial chemotherapy (76.2% and 65.9%, respectively).

4.4 *In vitro* analysis of hypoxia-related changes

4.4.1 Verification of the cell lines

We determined the expression of PAX5 and CD30 in the L1236 and L428 cell lines to provide evidence for the Hodgkin lineage. Both cell lines expressed the characteristic markers of cHL.

4.4.2 Expression of CAIX is induced by hypoxia

4.4.2.1 *Quantitative determination of CA9 expression*

The mRNA expression of CAIX was induced under hypoxia as compared to normoxia, however, the extent of induction was different. There was a 10-fold increase in the L1236 upon hypoxia, while there was a similar trend in the expression of the CAIX in L428 cells, but that did not reach statistical significance.

4.4.2.2 *Hypoxia induces the expression of CAIX*

Histological examination of the formalin-fixed cell lines specimens revealed that they have distinct expression patterns for the CAIX enzyme, which was in line with the RT-qPCR results. L428 showed only a minimal upregulation of the enzyme, while in the L1236 cell line the expression of CAIX proved to be highly inducible upon hypoxia. To semi-quantitatively analyze the samples, digital image analysis was applied. Slides were scanned with Panoramic MIDI Scanner and analyzed with the DensitoQuant algorithm. In normoxia, a little fraction of the pixels were positive for CAIX. In contrast, under hypoxia, almost 80% of the nuclei stained positive for CAIX.

4.4.2.3 Investigation of MIB1 activity and CAIX expression

We also examined the MIB1 expression in the case of the L1236 cell line to investigate the potential relationship between the proliferation index and CAIX expression (Figure 32.) similar to the retrospective clinical study. Double immunohistochemical staining was carried out to visualize the relation between MIB1 and CAIX.

Interestingly, we found that MIB1 and CAIX positivity may have an inverse relation, because the cells presenting with strong nuclear MIB1 positivity missed, or only minimally showed cell membrane CAIX expression. In contrast, large CAIX positive cells remained negative for the MIB1 immunostaining. The loss of proliferation potential may indicate that CAIX+ cells are about to enter a resting cellular state or cellular arrest as a response to hypoxia. The evaluation of CAIX and MIB1 double-stained slides included the relative quantification of the positive cells by counting. We classified the positive cells into 4 staging groups: double negative (CAIX- and MIB1-), double-positive (CAIX+ and MIB1+), CAIX positive (CAIX+ and MIB1-), and MIB1 (CAIX- and MIB1+) cells. We observed a significant decrease in the MIB1 activity consisted of CAIX-/MIB1+ and CAIX+/MIB1+ population in the samples treated in the hypoxia chamber compared to the normoxic control. As expected, the expression of CAIX was increased as CAIX+/MIB1- and CAIX+/MIB1+ fraction. The double-positive subpopulation might represent the cell compartment just finalizing cell cycle or cells with strongly reduced cell cycle duration. It is noteworthy, that the *in vitro* results are in line with previously published clinical data, as the reduced MIB1 activity was reported as a hallmark of the CAIX positive fraction in human malignancies.

4.4.2.4 Examination of dynamic CAIX expression

We assessed CAIX expression using flow cytometry which allowed the easy distinction of CAIX+ and CAIX- cell populations.

In L1236 cells the proportion of CAIX+ cells increased upon hypoxia. Our analyses showed, in normoxia there was a massive CAIX- cell population, and only a small number of cells expressed CAIX. However, in hypoxia, there was a drastic change in the distribution of the

cells. A shift into a CAIX positive range was observed and this result could indicate that the cells underwent a phenotypic change to survive in the hypoxic niche.

However, in L428 cells there was only a slight change in the proportions of CAIX+ cells.

4.4.2.5 Effect of cytotoxic treatment in L1236 cell line

Acetazolamide (AA) is a pharmacological inhibitor of CAIX.

To evaluate the potential effect of CAIX inhibition in our experimental model, we assessed whether AA treatment can modulate the response of *in vitro* cultivated cHL cells to the ABVD regimen. ABVD treatment induced cell death in L1236 cells under normoxia, while Hypoxia-induced the proportions of propidium iodide-positive cells that did not further increase upon ABVD treatment.

As we could not exclude the fact that the high cellular death could be due to the hypoxic microenvironment, we examined the effect of drugs in normoxic conditions and shorter incubation times. In the next experiment, we plated the cells a day before we treated them with ABVD mix and acetazolamide.

Next, we co-treated cultivated L1236 cells with ABVD and AA. In normoxia, AA did not induce cell death, while in combination with AVBD we observed increases in the proportions of propidium-iodide positive cells.

According to our results, the number of dead cells increased when AA was also applied to the treatment protocol, however, there was no significant difference between the MIX and MIX+AA groups.

Taken together, we propose that modulation of CAIX to cease enzyme activation may be a new therapeutic approach to increase the efficacy and efficiency of chemotherapeutic drugs.

5 Main findings

To briefly conclude, the main statements of the Ph.D. work are the following:

- The pathognomic cells of cHL, namely HRS-cells express CAIX. The expression of CAIX was selectively predominant on the HRS-cells.
- The expression of the enzyme was characteristic in the perinecrotic areas.
- Detection of CAIX expression has a predictive value for cHL progression and could predict the possible treatment response and outcome, thus as a potential biomarker, the usage of CAIX should be considered.
- The whole-slide digital analysis-based examination can detect the CD30 and CAIX positive cells and quantify the manner of their expression. CAIX positive cells are a subfraction of CD30 positive cells.
- L1236 showed a significant increase in CAIX expression upon hypoxia.
- According to our results, an increased CAIX expression is in an inverse correlation with MIB1 activity.
- It seems that CAIX expression may contribute to a cell cycle arrest, which could be a protective mechanism against hypoxia.

6 Publication list



UNIVERSITY of
DEBRECEN

UNIVERSITY AND NATIONAL LIBRARY
UNIVERSITY OF DEBRECEN
H-4002 Egyetem tér 1, Debrecen
Phone: +3652/410-443, email: publikaciok@lib.unideb.hu

Registry number: DEENK/481/2021.PL
Subject: PhD Publication List

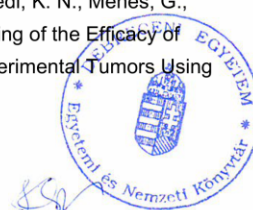
Candidate: Orsolya Matolay
Doctoral School: Doctoral School of Clinical Medicine

List of publications related to the dissertation

1. Méhes, G., **Matolay, O.**, Beke, L., Czenke, M., Jóna, Á., Miltényi, Z., Illés, Á., Bedekovics, J.:
Hypoxia related carbonic anhydrase IX expression is associated with unfavourable response to first-line therapy in classical Hodgkin's lymphoma.
Histopathology. 74 (5), 699-708, 2019.
DOI: <http://dx.doi.org/10.1111/his.13808>
IF: 3.626
2. **Matolay, O.**, Beke, L., Gyurkovics, A., Francz, M., Varjasi, G., Rejtő, L., Illés, Á., Bedekovics, J., Méhes, G.: Quantitative Analysis of Carbonic Anhydrase IX Uncovers Hypoxia-Related Functional Differences in Classical Hodgkin Lymphoma Subtypes.
Int. J. Mol. Sci. 20 (14), 1-12, 2019.
DOI: <http://dx.doi.org/10.3390/ijms20143463>
IF: 4.556

List of other publications

3. **Matolay, O.**, Bádon, E. S., Balázs, L., Juhász, P., Csonka, T., Méhes, G.: A szénsavanhidráz IX szerepe a malignus daganatok progressziójában - lehetséges terápiás célpont?
Magyar Onkol. 65, 157-166, 2021.
4. Kis, A., Dénes, N., Péli-Szabó, J., Arató, V. Z., Beke, L., **Matolay, O.**, Enyedi, K. N., Méhes, G., Mező, G., Bai, P., Kertész, I., Trencsényi, G.: In Vivo Molecular Imaging of the Efficacy of Aminopeptidase N (APN/CD13) Receptor Inhibitor Treatment on Experimental Tumors Using 68Ga-NODAGA-c(NGR) Peptide.
BioMed Res. Inter. 2021, 1-11, 2021.
IF: 3.411 (2020)





5. Méhes, G., **Matolay, O.**, Beke, L., Czenke, M., Pórszász, R., Mikó, E., Bai, P., Berényi, E., Trencsényi, G.: Carbonic Anhydrase Inhibitor Acetazolamide Enhances CHOP Treatment Response and Stimulates Effector T-Cell Infiltration in A20/BalbC Murine B-Cell Lymphoma. *Int. J. Mol. Sci.* 21 (14), 1-14, 2020.
DOI: <http://dx.doi.org/10.3390/ijms21145001>
IF: 5.923
6. Kis, A., Péli-Szabó, J., Dénes, N., Vágner, A., Nagy, G., Garai, I., Fekete, A., Szikra, D. P., Hajdu, I., **Matolay, O.**, Méhes, G., Mező, G., Kertész, I., Trencsényi, G.: In vivo Imaging of Hypoxia and Neoangiogenesis in Experimental Syngeneic Hepatocellular Carcinoma Tumor Model Using Positron Emission Tomography. *Biomed Res. Int.* 2020, 1-10, 2020.
DOI: <http://dx.doi.org/10.1155/2020/4952372>
IF: 3.411
7. Varga, G., Ghanem, S., Szabó, B., Nagy, K., Pál, N., Tánczos, B., Somogyi, V., Baráth, B., Deák, Á., **Matolay, O.**, Bidiga, L., Pető, K., Németh, N.: Which remote ischemic preconditioning protocol is favorable in renal ischemia-reperfusion injury in the rat? *Clin. Hemorheol. Microcirc.* 76 (3), 439-451, 2020.
DOI: <http://dx.doi.org/10.3233/CH-200916>
IF: 2.375
8. **Matolay, O.**, Méhes, G.: Sustain, Adapt, and Overcome: hypoxia Associated Changes in the Progression of Lymphatic Neoplasia. *Front Oncol.* 9, 1-7, 2019.
DOI: <http://dx.doi.org/10.3389/fonc.2019.01277>
IF: 4.848

Total IF of journals (all publications): 28,15

Total IF of journals (publications related to the dissertation): 8,182

The Candidate's publication data submitted to the iDEa Tudóstér have been validated by DEENK on the basis of the Journal Citation Report (Impact Factor) database.

29 October, 2021



Funding

Supported by the ÚNKP-20-3-II-DE-488, az ÚNKP-21-4-I-DE-253 New National Excellence Program of the Ministry of Innovation and Technology and EFOP-3.6.1-16-2016-00022 VENTURE CATAPULT, EFOP-3.6.3-VEKOP-16-2017-00009.

Acknowledgment

First of all, I would like to thank my supervisor, Gábor Méhes M.D., Ph.D., D.Sc, head of the Department of Pathology, University of Debrecen, Clinical Centre, for the patient guidance, encouragement, continuous support, and motivation during my Ph.D. study.

I would also like to thank Péter Bay, Ph.D., D.Sc. for allowing me to work at the Department. I am grateful that he gave me the opportunity to learn and work in his research group.

Many thanks to Edit Mikó Kapitányiné Ph.D, Judit Szabó Péliné M.Sc. for the valuable discussions and helpful advices. I am very grateful for Tünde Kovács Ph.D., Gyula Újlaki, Zsanett Mercédesz Sárközi Máténé Ph.D., Laura Jankó Ph.D. for their help in carrying out the experiments.

I am very thankful to Lívía Beke Mrs. for the immunohistological stainings.

My sincere thanks also go to György Vereb M.D., Ph.D., D.Sc, and István Rebenku M.Sc., who provided me an opportunity to join their team, and who gave me access to the laboratory and research facilities. Without their precious support, it would not be possible to conduct this research.

I would like to thank all of my former scientific students/TDK-students for joining me on this marvelous journey and for not only learning from me but teaching me: Áron Vajda M.D, Nóra Tárkányi M.D., Viktória Edina Kiss M.D, Szabolcs Viola, and Péter Dobi M.Sc, Ádám Fülöp.

Last but not least, I would like to show my gratitude towards my loving and supporting family and to all my dear friends for their continuous encouragement, support, and tolerance during my Ph.D. studies.